

Fall 2012

Structural Entropy and Metamorphic Malware

Donabelle Baysa
San Jose State University

Follow this and additional works at: https://scholarworks.sjsu.edu/etd_projects



Part of the [Computer Sciences Commons](#)

Recommended Citation

Baysa, Donabelle, "Structural Entropy and Metamorphic Malware" (2012). *Master's Projects*. 283.

DOI: <https://doi.org/10.31979/etd.6zrt-mb7y>

https://scholarworks.sjsu.edu/etd_projects/283

This Master's Project is brought to you for free and open access by the Master's Theses and Graduate Research at SJSU ScholarWorks. It has been accepted for inclusion in Master's Projects by an authorized administrator of SJSU ScholarWorks. For more information, please contact scholarworks@sjsu.edu.

Structural Entropy and Metamorphic Malware

A Project

Presented to

The Faculty of the Department of Computer Science

San Jose State University

In Partial Fulfillment

of the Requirements for the Degree

Master of Science

by

Donabelle Baysa

May 2013

© 2013

Donabelle Baysa

ALL RIGHTS RESERVED

The Designated Project Committee Approves the Project Titled

Structural Entropy and Metamorphic Malware

by

Donabelle Baysa

APPROVED FOR THE DEPARTMENTS OF COMPUTER SCIENCE

SAN JOSE STATE UNIVERSITY

May 2013

Dr. Mark Stamp Department of Computer Science

Dr. Robert Chun Department of Computer Science

Dr. Richard Low Department of Mathematics

ABSTRACT

Structural Entropy and Metamorphic Malware

by Donabelle Baysa

Metamorphic malware is capable of changing its internal structure without altering its functionality. A common signature is nonexistent in highly metamorphic malware. Consequently, such malware may remain undetected even under emulation and signature scanning combined.

In this project, we use the concept of structural entropy to analyze variations in the complexity of data within a file. The process consists of two stages, namely, file segmentation and sequence comparison. In the file segmentation stage, we use entropy measurements and wavelet analysis to segment a file. The second stage measures the similarity of files by computing the edit distance between sequence segments. We apply this technique to the metamorphic detection problem and show that we can obtain strong results in certain challenging cases.

ACKNOWLEDGMENTS

My sincere appreciation is due to my advisor, Dr. Mark Stamp, for his guidance and encouragement throughout the project. I consider it an honor to have worked with a professor who possesses true passion for teaching.

I would like to thank my committee members, Dr. Robert Chun and Dr. Richard Low, for their contribution in the completion of this project.

I would like to express my earnest love and gratitude to my husband, Mark, for his unconditional support and understanding through the duration of my studies. A special recognition goes to my 2-year old daughter, Olivia, who keeps my work-life balance in-check. Finally, I would like to thank my mom, Cynthia, for her continued support and praises.

TABLE OF CONTENTS

CHAPTER

1	Introduction	1
2	Background	3
2.1	Malware	3
2.1.1	Viruses and worms	4
2.1.2	Obfuscation techniques	4
2.2	File similarity methods	7
2.2.1	HMM-based detection	7
2.2.2	Similarity index	9
2.2.3	Opcode graph-based similarity	10
2.3	Structural entropy	11
3	Design	13
3.1	File segmentation	13
3.1.1	Wavelet transform analysis	14
3.1.2	Segmentation using wavelet transform	15
3.2	Sequence comparison	18
3.2.1	Levenshtein distance	18
3.2.2	Sequence alignment using Levenshtein distance	19
3.2.3	Similarity calculation	22
4	Experiments	24
4.1	Test data	25

4.2	Parameters	26
4.3	Results	27
5	Conclusion and Future Work	36
APPENDIX		
A	MWOR Results	41
B	NGVCK Results	45
C	ROC Curves	47

LIST OF TABLES

1	An example of instruction transposition	6
2	Edit matrix for strings “eleven” and “elevated”	20
3	Cygwin files from ./cygutils	25
4	Linux system files	26
5	MWOR 0.5 similarity statistics	29
6	MWOR similarity statistics	30
7	AUC of NGVCK	33

LIST OF FIGURES

1	“Do-nothing” instructions [29]	7
2	Generic Hidden Markov Model [20]	8
3	Similarity index [28]	10
4	Transform assembly instructions to weighted directed opcode graph [15]	11
5	Basic executable file format	14
6	Wavelet and signal under investigation [1]	15
7	File segmentation process	16
8	Entropy plot of a sample file	17
9	Wavelet transform of a sample file	17
10	Penalty cost for the entropy difference between two segments	21
11	Sequence comparison process	23
12	G2 similarity	28
13	MWOR 0.5 similarity	29
14	NGVCK (4 KB) similarity	31
15	NGVCK (8 KB) similarity	32
16	NGVCK (4 KB and 8 KB) similarity	32
17	NGVCK ROC curves	33
18	AUC for NGVCK with various parameter values	34
19	File processing time	35

CHAPTER 1

Introduction

Metamorphism is a technique applied to computer programs in order to change its internal structure while maintaining its functionality. It is popular among malware writers for its effectiveness at evading detection by traditional signature-based anti-virus software. As a result, well-written metamorphic viruses have the potential to remain undetected. Therefore, static methods for measuring file similarity is of interest.

Previous research projects [12, 15, 28] aimed at metamorphic detection based on static analysis of files have shown promising results against metamorphic malware, including the highly metamorphic family of viruses produced by the NGVCK (Next Generation Virus Creation Kit) generator.

This research project introduces a file similarity method based on the paper [17], which utilizes static analysis to measure the similarity of executable files. The technique uses the concept of structural entropy to analyze the complexity of a file's data order. This method consists of two stages, namely, file segmentation and sequence comparison. In the file segmentation stage, we use entropy measure and wavelet analysis to segment a file. The second stage estimates the similarity of files by using the edit distance between sequence segments. We apply this approach to identify whether a given file belongs to a known metamorphic malware family.

The information in this report is presented as follows. Section 2 includes discussion of previous research projects related to file similarity measure. We review a solution that uses Hidden Markov Models [28], a method based on graph analysis [15],

and a similarity index [28] technique. We also present background information on malware and briefly introduce the concept of structural entropy, which is the basis of our similarity measure. Section 3 describes the design of our method. In Section 4, we show the results of our solution when applied to the metamorphic malware detection problem. Finally, in Section 5 we convey our conclusions and propose direction for future work.

CHAPTER 2

Background

Development of methods for estimating file similarity is an important topic in virus detection. Advanced anti-virus (AV) schemes such as emulation are often employed in conjunction with static signature-based detection to scan for more sophisticated viruses that employ obfuscation techniques such as encryption, polymorphism, and metamorphism. However, the overhead (e.g., file storage spaces and resources) and the complexity of these techniques pose challenges to AV vendors. Additionally, as we will discuss in Section 2.1.1, metamorphic malware may remain undetected even under the scrutiny of code emulation and signature-based detection. One solution to these problems is static analysis of files. It defines file characteristics needed for comparison without examining its functionality, thereby eliminating the emulation process and in turn, reduces implementation difficulty. Also, it is purely based on the analysis of different areas of a file which makes it resilient to techniques used by malware writers to protect their code.

First, we provide background information on malware including the methods it uses to avoid detection. Then, we review other file similarity measures which were applied to the metamorphic malware detection problem. Then we briefly discuss the concept of structural entropy and describe how we apply it to our similarity method.

2.1 Malware

Malware is a computer program designed to cause harm to computer systems. It interrupts normal computer operation, destroys files by infection or deletion, steals user information, and damages system resources such as the hard disk [25]. It enters

the system without user consent. Malware comes in various forms such as virus, worm, trojan horse, and other programs created with malicious intent. In this paper, we only consider viruses and worms.

2.1.1 Viruses and worms

A computer virus is a malware that executes itself by embedding its code to another executable program. When the infected program executes, it, in turn, infects other files, corrupting the host system. Thus, viruses are self-replicating programs that cause destruction within the host machine [19, 25].

In contrast to viruses, worms do not require other executable files to cause intrusion. That is, they are standalone programs. A worm spreads itself from one system to another on the network [25]. Worms not only have the ability to damage its host system but also cause disruption to the computer networks.

Viruses and worms use a number of obfuscation techniques to avoid signature-based detection. The aim is to make itself look different at each replication, making it difficult for a scanner to find commonalities between the variants. To achieve this, malware writers use methods such as encryption, polymorphism, and metamorphism [28]. In the next sections, our discussion will focus on viruses. However, these topics also apply to computer worms.

2.1.2 Obfuscation techniques

Encryption is the simplest form of code obfuscation. The virus body is encrypted using a key. Given that a different encryption key is used in each generation, the virus variants will not share a common pattern necessary for signature scanning, thereby evading detection. The virus also includes a decryptor module which decrypts

the virus body at execution. The decryptor is usually a simple, decrypted piece of code that remain constant across replications [29]. Therefore, the decryptor code is susceptible to detection.

Polymorphism is a step up to encryption, which possesses vulnerability to detection. That is, an encrypted virus carries a detectable decryptor code. A polymorphic virus not only uses encryption to hide its virus body, it also mutates its decryptor so that each virus variant looks different from one another [11, 29]. Therefore, no common pattern exists that will allow signature scanners to use for identification. However, just as malware writers use sophisticated methods to evade detection, AV software vendors develop other means to defeat them. In conjunction with signature scanning, AV vendors use code emulation to allow potential viruses to execute in a protected environment. Once the virus decrypts itself within this virtual environment, it exposes its virus body, which stays constant, to detection.

Metamorphic virus goes even further and mutates its entire virus body, making it resistant to emulation. A virus using metamorphism changes its internal structure in each replication while maintaining its functionality [11, 29]. A highly metamorphic virus does not necessarily need encryption since each generation will produce a structurally different code and retrieval of a common signature will be highly unlikely [19]. Therefore, encryption adds no benefit to the virus creation. As such, a well developed metamorphic virus has the potential to remain undetected.

There are a number of techniques to create mutated virus programs. One simple method is to apply register swapping. In this approach, the code remains unchanged except for the registers. For example, `ADD EDX,0088h` can be converted to `ADD EAX,0088h`, i.e., the register `EDX` is swapped for `EAX`. However, register swapping can typically be exploited by a wildcard string [12].

Another prevalent method used in metamorphism is equivalent instruction substitution. An instruction or a set of instructions is exchanged for another yielding the same result. For example, the sequence of instructions `PUSH R1; MOV R1,R2` can be substituted for `PUSH R1; PUSH R2; POP R1`, which results in the same functionality [28].

In some instances, the order of instructions can be rearranged without losing the functionality if the instructions have no dependency with each other. This technique is called instruction transposition; it enables viruses avoid signature-based detection since the order of bytes deviates in each replication [19]. A simple example of this method is shown in Table 1.

Table 1: An example of instruction transposition

Original Instructions	Transposed Instructions
1: SUB R1, R2	1: SUB R3, R4
2: SUB R3, R4	2: SUB R1, R2

Subroutine permutation is another technique for manipulating the internal structure of a virus without changing the functionality. With n subroutines in a virus, $n!$ variants of the virus can be generated. A virus with 10 subroutines, like the Win32/Ghost virus, can easily generate $10!$ or 3,628,800 versions of itself [29]. However, since the subroutines do not change, using this method alone can expose the virus to detection by searching for common short string patterns [28].

Garbage instruction insertion is an effective metamorphic technique. Garbage instructions are those that are either executed without impacting the virus behavior, or skipped all together. The former type of garbage instructions are often referred as “do-nothing” code, and the latter are “dead-code” instructions. An example of a

“do-nothing” code sequence is shown in Figure 1.

00401005	8BF0	MOV ESI,EAX
00401007	3E:8A00	MOV AL,BYTE PTR DS:[EAX]
0040100A	84C0	TEST AL,AL
0040100C	74 4D	JE SHORT Test.00401058
0040100E	53	PUSH EBX
0040100F	3E:8F05 74F940	POP DWORD PTR DS:[40F974]
00401016	D3DB	RCR EBX,CL
00401018	0FCB	BSWAP EBX
0040101A	68 5D104000	PUSH Test.0040105D
0040101F	58	POP EBX
00401020	3E:8903	MOV DWORD PTR DS:[EBX],EAX
00401023	43	INC EBX
00401024	0FBDC2	BSR EAX,EDX
00401027	A9 46A978DC	TEST EAX,DC78A946
0040102C	8BC2	MOV EAX,EDX
0040102E	90	NOP
0040102F	90	NOP
00401030	42	INC EDX
00401031	52	PUSH EDX
00401032	FE0C24	DEC BYTE PTR SS:[ESP]
00401035	4A	DEC EDX
00401036	B6 86	MOV DH,86
00401038	B3 27	MOV BL,27
0040103A	B8 7CFAA17F	MOV EAX,7FA1FA7C
0040103F	EB 01	JMP SHORT Test.00401042
00401041	90	NOP
00401042	0FBCC2	BSF EAX,EDX
00401045	3E:C705 FC8841	MOV DWORD PTR DS:[4188FC],0
00401050	2D 210DE8B9	SUB EAX,B9E80D21
00401055	69DA E577D49D	IMUL EBX,EDX,9DD477E5

Figure 1: “Do-nothing” instructions [29]

2.2 File similarity methods

In this section, we review previous research projects designed for estimating file similarity between samples from a number of metamorphic family of viruses.

2.2.1 HMM-based detection

A hidden Markov model (HMM) represents a system having a Markov process in which the states are non-observable [9, 20]. In other words, the process of transitioning from one state to the next is dependent only on the current state and each state in the transition sequence is hidden. What is visible, however, is the series of output observed during the transition process [20, 28]. Figure 2 shows a generic HMM. Here, the Markov process consists of X_t hidden states which are “driven” by the state transition probabilities A . Each hidden state uncovers some information, i.e., observation O_t , over a probability distribution B . Therefore, given a sufficient sample of observations, we can produce a model that represent the data sample maximally.

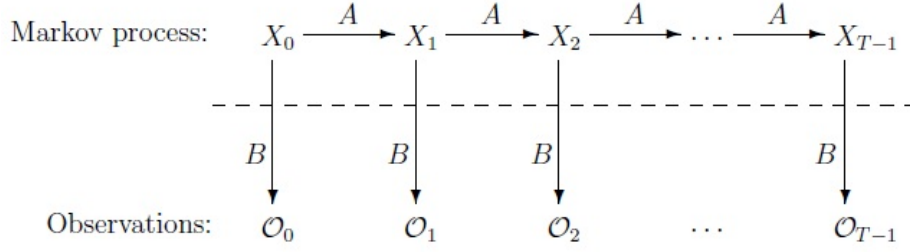


Figure 2: Generic Hidden Markov Model [20]

We can then determine if another given set of data is related to the observed data represented by the model. Generating a system that models a sample data set and utilizing it to expose data relationships are two of the three fundamental problems that can be solved using HMMs [20]. We can also discover the unknown states of the HMM given the model and a set of data. For more details on HMM, refer to [20].

The paper [28] presents a detector based on hidden Markov models (HMM) and shows superiority over popular commercial virus scanners on a set of test files. The HMM method effectively detects metamorphic viruses produced by various metamorphic generators including NGVCK, which generates highly morped versions of a given virus. The technique involves training and detection phases. The training phase generates a hidden Markov model on a given file set of a metamorphic virus family (e.g., NGVCK). The model is trained on the assembly opcode sequences of the viruses. The process starts by disassembling the virus executable files, producing assembly opcodes, which are then concatenated into a long sequence of opcodes that is used to build the model. The result is a model that represents the statistical profile of the virus family. In order to classify a given file as being malicious or benign, the resulting HMM is used to measure the log likelihood of the virus files in the test set, which belongs to the same virus family used in the training phase. The expectation is that the model would give high likelihood scores to these files. The same calculation

is performed on another set consisting of normal files and virus files from another virus family. The goal is to clearly set distinctions between “family viruses”, “non-family viruses”, and “normal files”. The results show that the HMM method is highly effective at detecting family viruses, overpowering some commercial virus scanners.

2.2.2 Similarity index

The same paper [28] presents another similarity measure based on similarity index. Although the technique is simpler, it is equally effective at detecting metamorphic viruses. In fact, the experiment resulted in 100% detection rate and 0% false positive rate. Similar to the HMM approach, this method analyses the opcode sequences of files. However, here it directly compares the opcode sequences of two files by matching all three consecutive opcode subsequences from each, in any order. For example, an opcode sequence of [add, sub, mov] from one file matches the following sequences from another file: [sub, mov, add], [mov, add, sub], and [sub, add, mov]. The matching subsequences are then plotted and adjusted, based on a threshold, to cut down random matches. By reducing noise, the graph shows a more accurate representation of the matching sequences. Figure 3 illustrates this process. The similarity score is calculated based on the average of real matches. The file being examined is categorized as “non-family” if it has no similarity to a randomly chosen virus file from a known virus family. Otherwise, additional comparisons are required between the chosen virus file and other files from the same virus family to set a threshold. If the similarity score between the given file and the originally chosen virus file is above the threshold, the file is deemed a “family” virus.

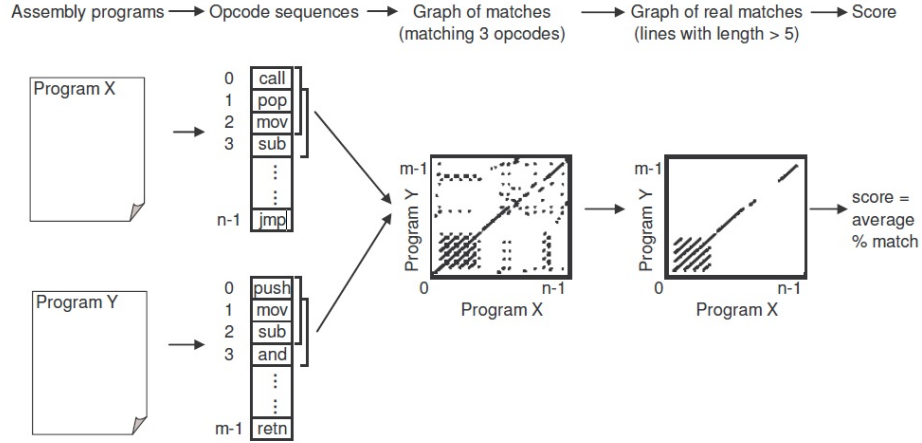


Figure 3: Similarity index [28]

2.2.3 Opcode graph-based similarity

In a more recent work, a technique developed using opcode graph [15] outperforms the HMM-based detection under certain scenarios. This method takes an executable file, disassembles it, and extracts the opcode sequence. The sequence is then transformed into a weighted directed graph. The graph is constructed as follows. The nodes represent all the distinct opcodes. An edge is added from each opcode node to all of its successor opcode nodes. The probability of the successor opcode node is assigned as the weight of the corresponding edge. Figure 4 shows an example of a weighted opcode graph of a sample assembly instructions.

To compare two files, the opcode graph is built for each file. The generated opcode graphs are compared directly via a scoring function which takes the corresponding edge weights (probabilities of two opcodes or itself occurring in sequence) from the two opcode diagrams and calculates a similarity score. This process is performed on pairs of virus files from a metamorphic virus family. The expectation is to get scores with little to no variations from these family viruses. Similarly, the score

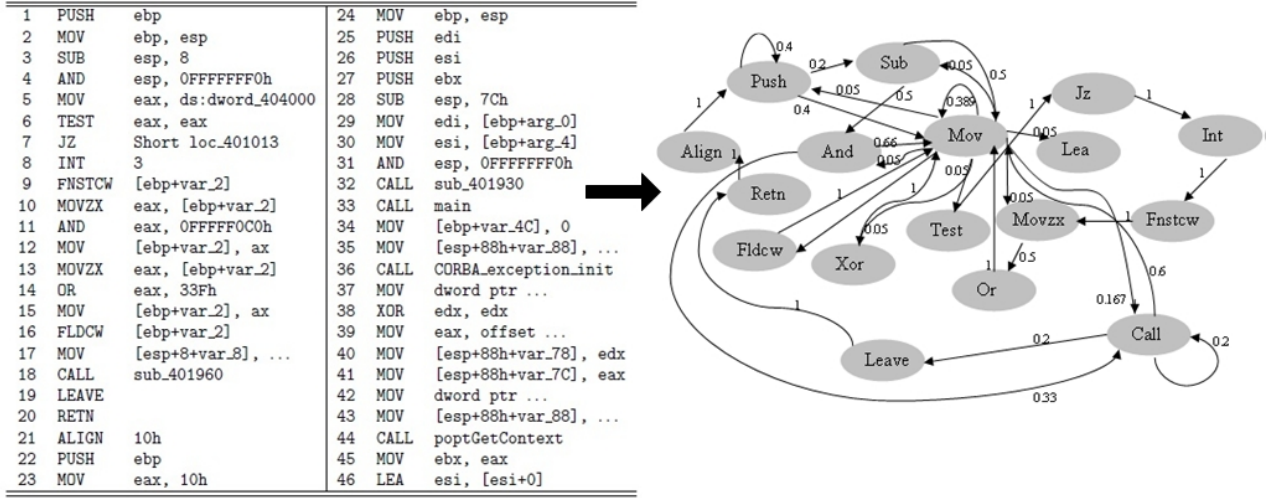


Figure 4: Transform assembly instructions to weighted directed opcode graph [15]

calculation is performed on file pairs involving one virus file from the same metamorphic family used in the earlier computation, and one benign file from a sample set of normal files. A threshold is set based on these score calculations.

Finally, in order to detect a given file, its opcode graph is compared against an opcode graph from a metamorphic virus family used in the above calculations. Depending on where the score falls with respect to the threshold, it is classified as a member of the metamorphic virus family or benign.

2.3 Structural entropy

Entropy is “a statistical measure of the disorder of a closed system” [5]. It quantifies uncertainty of systems where outcomes are not equally likely [8]. Our solution focuses on the order of code and data areas of a file, characterizing it by the peculiarity of its byte sequences as well as its length. We use entropy measurement to find distinctions of bytes within the file. This technique is derived from the paper [17] which produced efficient and favorable experimental results on polymorphic malware

samples. In this project, we apply it to the metamorphic detection problem.

We use the concept of structural entropy to analyze the complexity of a file's data order. It consists of two stages, namely, file segmentation and sequence comparison. In the file segmentation stage, we use entropy measurement and wavelet analysis to segment a file. The second stage measures the similarity of files by using the edit distance between sequence segments.

CHAPTER 3

Design

As previously cited, the similarity method we consider here is derived from the paper [17]. It is based upon static analysis of files using structural entropy to measure similarity between two files. In contrast to [15, 28], this solution examines executable files without code disassembly. Instead of analyzing opcode sequences of files, we scan the binaries directly and observe the distinctions of each byte with respect to one another for different areas within the files. In other words, we are only interested in the structure, specifically, entropy and size characteristics of a file.

The proposed solution compares two given files and produces a similarity measure. It starts by splitting each file into sequence of segments of different entropy levels using entropy and wavelet analysis, followed by aligning the two sequences by calculating the edit distance between the sequence segments. The result is the similarity between the two files, expressed as a percentage.

3.1 File segmentation

The key in properly segmenting a file is to locate the areas where significant changes occur. In our method, we are looking directly into the sequence of data bytes within an executable file. The standard structure of an executable includes information about its code and data fragments. Figure 5 shows a basic format of a Windows portable executable file, organized into various sections [7, 13, 14]. The format starts with structures of different headers followed by the code and data regions. Each of these file fragments can be characterized by the nature of information it contains. For instance, the header sections include pointers to other areas within the file, and the

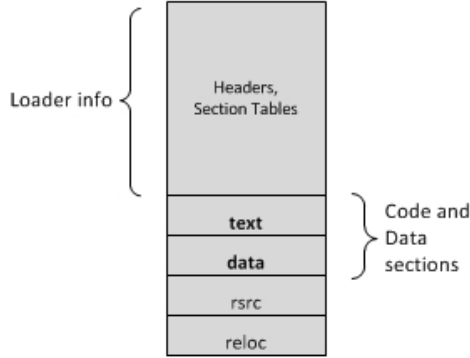


Figure 5: Basic executable file format

text and data sections contain the code and initialized data (i.e., initialized global and static variables), respectively [13, 14, 16]. The method we use here is based on the notion that variants from the same malware family will share similar code patterns and data structures in order to preserve its malicious intent. Therefore, we can examine not only the similarity within the headers, but more importantly, the distinctive byte sequences within the code and data sections. We can use entropy and size to represent each of these byte patterns and use them as bases for our file segmentation process. Consequently, our goal is to find the borders where these areas occur and use it to segment a file. We achieve this by using wavelet analysis on a file represented as a series of entropy measure.

3.1.1 Wavelet transform analysis

Wavelet analysis is a process of transforming a signal (i.e., a data set) into a more revealing and useful form. It uses wavelets, which are wavelike functions, to analyze the raw data in different locations and for different wavelet scales [1, 21]. Figure 6 illustrates the signal and the analyzing wavelet. The transformation at a given scale is determined based on the signal approximation and detail at the previous scale.

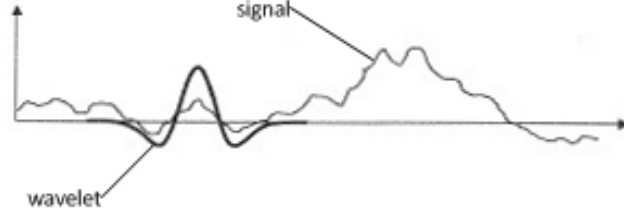


Figure 6: Wavelet and signal under investigation [1]

Scaling the wavelet smooths out the high frequency information present in the original data. The transformed data is referred as *wavelet transform*, which represents the relationship of the data and the analyzing wavelet. Mathematically, it is a convolution of the signal and the wavelet function for a range of locations and scales [1].

3.1.2 Segmentation using wavelet transform

We use wavelet analysis to trace those areas in the file where significant changes occur. The process is as follows. First, we apply the sliding window method to represent the file as a series of entropy measures $Y = \{y_i : i = 1, \dots, N\}$, where N is the number of windows and y_i is the entropy of each window. The entropy is calculated using Shannon's formula [3]

$$y_i = - \sum_{j=1}^m p(j) \log_2 p(j), \quad (1)$$

where $p(j)$ is the frequency of byte j within window i , and m is a number of distinct bytes in the window. Second, the resulting entropy series Y is fed into wavelet analysis using discrete wavelet transform

$$W(a, b) = \frac{1}{|a|^{1/2}} \sum_{i=1}^N y_i \psi_{HAAR} \left(\frac{t_i - b}{a} \right), \quad (2)$$

where a is a scaling parameter, b is a shifting parameter of the analyzing wavelet, y_i is the entropy of window i , N is the number of windows in the file, and ψ_{HAAR} is the

Haar wavelet function, which is defined by

$$\psi_{HAAR}(t) = \begin{cases} 1, & 0 \leq t < 1/2, \\ -1, & 1/2 \leq t < 1, \\ 0, & t < 0, t \geq 1. \end{cases}$$

The wavelet transform formula in (2) requires the scaling parameter a to be of power of 2, i.e., $a_n = 2^n$ where n is the maximum scale index [26]. For example, if we want to transform the raw data to the maximum scale of 16, equation (2) will be iterated four times for $a = 2, 4, 8$, and 16 and for different locations, b , on the data. The file segments are determined by the wavelet coefficients at the maximum scale, where boundaries of these segments are defined by the local extrema based on a set threshold. The file segmentation process is summarized in Figure 7.

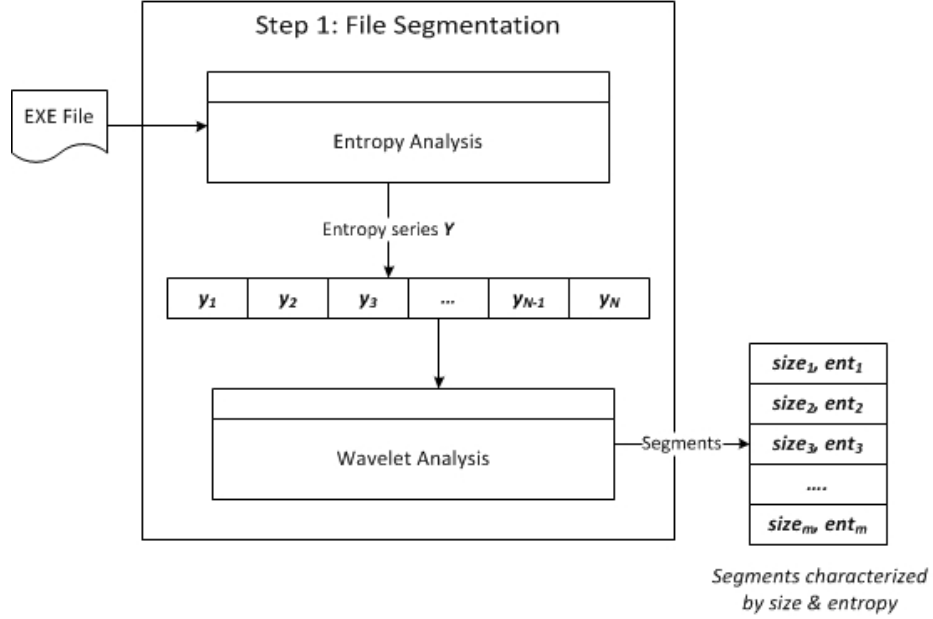


Figure 7: File segmentation process

To illustrate our file segmentation method, consider the diagram in Figure 8, which shows the entropy plot of a 4 KB size sample file. This entropy series is calculated using a window size and window slide size of 64 bytes and 32 bytes, respectively.

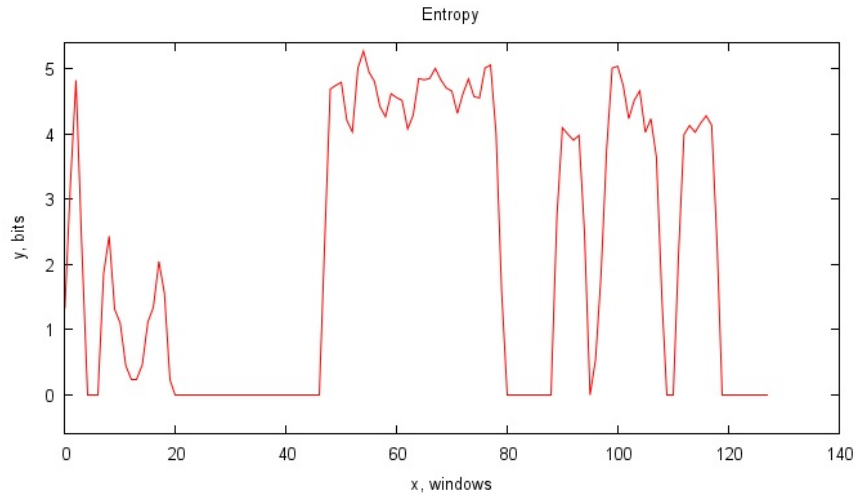


Figure 8: Entropy plot of a sample file

Using 32 bytes for the slide size ensures the entropy map size to be of power of 2, which is 128 in this example. The wavelet transform of this sample file is shown in Figure 9 with maximum scale of 16, i.e., $a_4 = 2^4$. On the lower transformation scales,

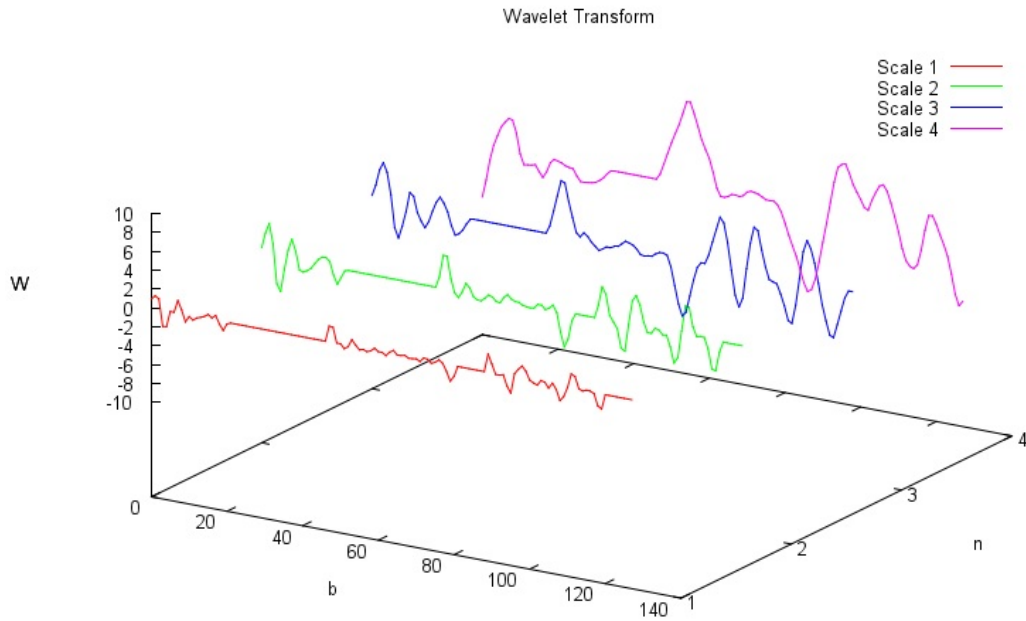


Figure 9: Wavelet transform of a sample file

detail of changes in source data is evident, while insignificant changes are ignored at the higher scales. Therefore, the segments are determined by the coefficients at scale index 4. Using a threshold, we can locate the segment borders by finding peaks that are greater than the threshold in height.

3.2 Sequence comparison

Once each file has been transformed into a sequence of segments, we compare the two sequences and determine the degree of similarity between them. The comparison process is as follows. First, we align the two sequences by evaluating the differences of their respective elements. We achieve this by using an algorithm based on the Levenshtein distance. The result is a measure of the difference between two sequences [10]. We then use this result to estimate the similarity between the two files.

In this section, we first provide background information on the Levenshtein distance. Then we illustrate how it is used in our sequence alignment algorithm. Finally, we discuss our method for evaluating the similarity measure.

3.2.1 Levenshtein distance

The Levenshtein distance, or edit distance, is a measure of the difference between two sequences of data [10]. It calculates the distance by tallying the minimum number of edit operations required to transform the first sequence into the other. The set of edit operations are substitution, insertion, and deletion. Substitution replaces an element from the first sequence with an element in the second sequence, insertion adds a element into the second sequence, and deletion removes an element from the second sequence [2, 27]. Each required edit operation adds to the overall distance. In other words, each edit translates into a penalty. Consequently, the more the edits,

the higher the difference is between two sequences.

Consider an example of comparing two sequences of characters where each substitution, insertion or deletion results to a penalty of 1. The number of edit operations required to transform the string “eleven” to “elevated” is 3,

1. eleven \rightarrow eleva**e**n, *insert ‘a’*
2. elevaen \rightarrow elevat**e**n, *insert ‘t’*
3. elevaten \rightarrow elevated**d**, *substitute ‘n’ for ‘d’*.

Notice that the transformation cannot be completed in fewer than three edits, therefore the Levenshtein distance between these two strings is 3.

Equation 3 formulates the general definition of the Levenshtein distance $D(i, j)$ between sequences $x[1 : m]$ and $y[1 : n]$ where edit penalties are determined by the cost function δ [2].

$$D(i, j) = \begin{cases} 0 & \text{if } i = 0 \text{ and } j = 0 \\ D(0, j - 1) + \delta(\lambda, y_j) & \text{if } i = 0 \text{ and } j > 0 \\ D(i - 1, 0) + \delta(x_i, \lambda) & \text{if } i > 0 \text{ and } j = 0 \\ D(i - 1, j - 1) & \text{if } x_i = y_j \\ \min \begin{cases} D(i, j - 1) + \delta(\lambda, y_j) \\ D(i - 1, j) + \delta(x_i, \lambda) \\ D(i - 1, j - 1) + \delta(x_i, y_j) \end{cases} & \text{if } x_i \neq y_j. \end{cases} \quad (3)$$

Applying this definition to our previous example with $\delta = 1$ (i.e., penalty is 1) for each edit operation produces the edit matrix in Table 2. The last matrix element represent the edit distance, which is 3 in our example.

3.2.2 Sequence alignment using Levenshtein distance

As discussed in the the previous section, the Levenshtein distance adds a penalty of 1 on each edit operation applied on sequences of characters. In our method, we

Table 2: Edit matrix for strings “eleven” and “elevated”

		e	l	e	v	a	t	e	d
	0	1	2	3	4	5	6	7	8
e	1	0	1	2	3	4	5	6	7
l	2	1	0	1	2	3	4	5	6
e	3	2	1	0	1	2	3	4	5
v	4	3	2	1	0	1	2	3	4
e	5	4	3	2	1	1	2	2	3
n	6	5	4	3	2	2	2	3	3

are dealing with sequence elements that are characterized by size and entropy. Thus, our cost function must penalize on the difference of two elements based on their sizes and entropy values. As in [17], we choose the function for calculating the size penalty

$$\text{cost}_s(x, y) = \frac{|x.\text{size} - y.\text{size}|}{x.\text{size} + y.\text{size}}, \quad (4)$$

where x and y are the two compared segments. If they are equal in size, the penalty is 0. The maximum size penalty, in the case of absolute difference, is 1.

For evaluating the difference in entropy, we use the equivalent formula in [17] based on a Sigmoid function

$$\text{cost}_e(x, y) = \frac{1}{1 + \exp(-4 \cdot |x.\text{ent} - y.\text{ent}| + 6.5)} - 0.001501, \quad (5)$$

where each segment is associated with an entropy value denoted by “ent”. Function (5) represents a sigmoid curve [23], as shown in Figure 10. The use of constants, 6.5 and 0.001501, in equation (5) forces the cost to equate to 0 when the entropy difference of two segments is 0. As with the size, the maximum entropy penalty is 1. Adding the size (4) and entropy (5) costs gives us the total penalty

$$\text{cost}(x, y) = \text{cost}_s(x, y) \cdot \text{PART_SIZE} + \text{cost}_e(x, y) \cdot \text{PART_ENT}, \quad (6)$$

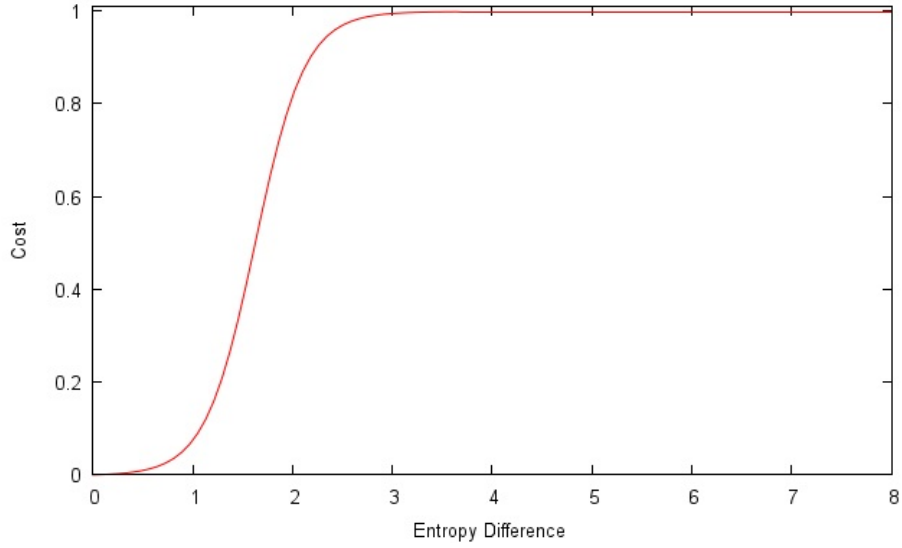


Figure 10: Penalty cost for the entropy difference between two segments

where `PART_SIZE` and `PART_ENT` are used to allow the penalty fractions to be set differently.

Now that we have determined a cost function (6), we apply it into our sequence alignment algorithm based on Levenshtein distance, which builds a two-dimensional edit array d using dynamic programming where each of its element is determined by the preceding elements. At each step of filling in this array, we will use the cost function (6), which penalizes based on the size and entropy differences, as well as the logarithmic sizes of the compared segments. The resulting penalty for comparing two sequences s_1 and s_2 is determined by the last element in the d matrix.

For the first column of d , we use the formula

$$d[i][0] = d[i-1][0] + \text{TAX} \cdot \log_{10}(s_1[i-1].\text{size}), \quad i = 1 \dots \text{length}(s_1),$$

which corresponds to deletion of elements from the first sequence s_1 . The constant `TAX` allows for adjustment to the penalty calculation. Similarly, we use the formula

for filling in the first row

$$d[0][j] = d[0][j - 1] + \text{TAX} \cdot \log_{10}(s_2[j - 1].\text{size}), \quad j = 1 \dots \text{length}(s_2),$$

which denotes insertion of elements from the second sequence s_2 . The rest of the elements are set using the formula

$$d[i + 1][j + 1] = \min \begin{cases} d[i][j] + \text{cost}(s_1[i], s_2[j]) \cdot \log_{10}((s_1[i].\text{size} + s_2[j].\text{size})/2) \\ d[i][j + 1] + \text{TAX} \cdot \log_{10}(s_1[i].\text{size}) \\ d[i + 1][j] + \text{TAX} \cdot \log_{10}(s_2[j].\text{size}). \end{cases} \quad (7)$$

For each remaining item of d , we calculate the three equations in (7) and select the minimum result. The penalty for substituting an element from s_1 to an element in s_2 is given by the first equation in (7). In this case, we take into account both the overall cost (6) and the average size of the two segments. The second equation evaluates the penalty for a deletion of an element in sequence s_1 . Lastly, an insertion of an element into sequence s_2 is specified by the third equation. Penalties from both the deletion and insertion operations are based on the size of the segment.

3.2.3 Similarity calculation

Using the resulting edit distance (i.e., the last element of the edit matrix d) as described in the previous section, we can then calculate the similarity percentage between s_1 and s_2 sequences by the formula

$$\text{similarity} = 100 - \frac{d[\text{length}(s_1)][\text{length}(s_2)]}{\text{cost}_{\max}} \times 100, \quad (8)$$

where cost_{\max} is the penalty in the worst case scenario where all elements in s_1 are deleted and all elements in s_2 are inserted. In addition, we increase this penalty based on the edit operation being performed. This maximum penalty is determined

as follows

$$\text{cost}_{max} + = \begin{cases} 2 \cdot \text{TAX} \cdot (\log_{10}(s_1[i].\text{size}) + \log_{10}(s_2[j].\text{size})), & s_1[i] \text{ substitute } s_2[j] \\ \text{TAX} \cdot \log_{10}(s_1[i].\text{size}), & \text{delete } s_1[i] \\ \text{TAX} \cdot \log_{10}(s_2[j].\text{size}), & \text{insert } s_2[j]. \end{cases} \quad (9)$$

Calculating cost_{max} is similar to penalty calculations for the first column and first row of matrix d . The only exception is the doubling of the penalty when the element from the sequence s_1 is substituted for the element in the second sequence s_2 .

Figure 11 summarizes the comparison of two sequences of file segments.

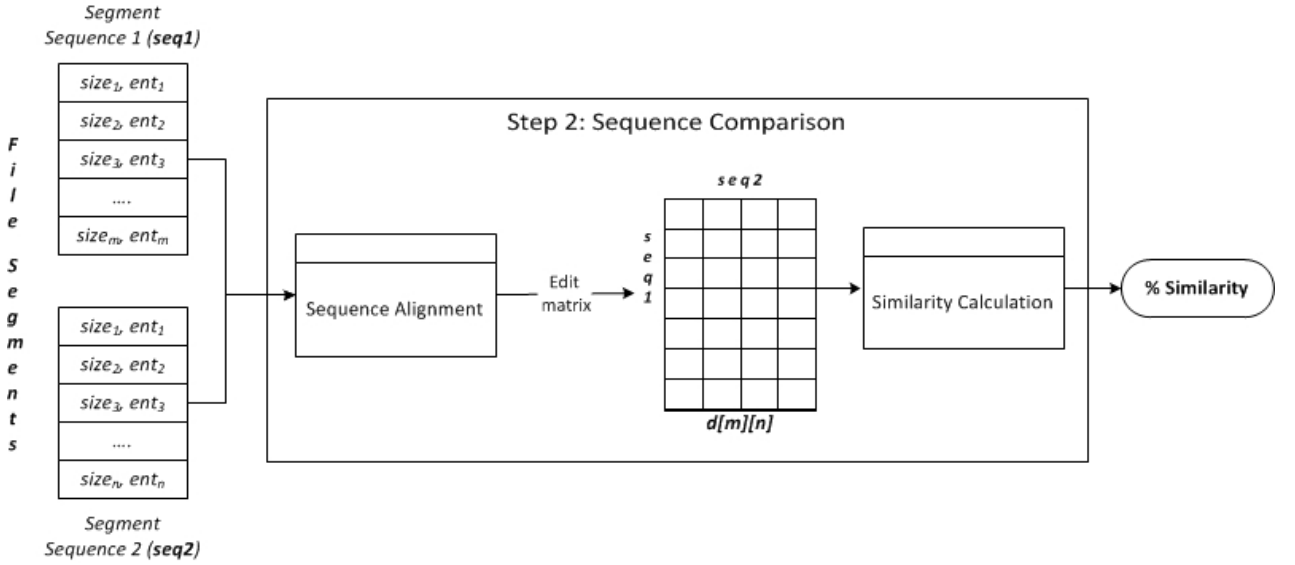


Figure 11: Sequence comparison process

CHAPTER 4

Experiments

We apply our method to the metamorphic virus detection problem using a process consistent with [15] with a slight alteration. The difference is in the number of comparisons, i.e., pairing of files. Instead of exclusive pairing [15], we compute the similarity of each possible pair in the test set. This progression from [15] makes for a more complete experiment, hence produce a more accurate result.

In order to identify malicious programs, we define a similarity threshold that separates them from the benign programs. Our goal is to clearly distinguish the viruses from ordinary files. To set the threshold, we perform the following steps:

1. Determine the similarity range for a metamorphic virus family by calculating the degree of similarity for all pairs of virus files. For a test set of 50 files, as in the case of the G2 and NGVCK family of viruses, we will perform $\binom{50}{2}$ similarity calculations, which is equivalent to 1,225 comparisons.
2. Determine the similarity range for the metamorphic files used in step 1 versus a set of benign files by calculating the degree of similarity for all pairs. For a set of 50 virus files and 16 benign files, this will generate $(50 * 16) = 800$ comparisons.
3. Set the threshold by analyzing the values around the lower end of the range in step 1 and higher end of step 2.

If a threshold can be set in step 3, then our method is capable of detecting a virus from a known metamorphic virus family.

4.1 Test data

We use 50 virus files generated by G2 (Second Generation virus generator) and 50 files from the NGVCK virus family [24]. For the comparison set (i.e., benign files), we use 16 randomly selected Cygwin utilities files [4] shown in Table 3. The Cygwin files are chosen with the assumption that much of their functionality is comparable with those of the virus programs without the malicious intent. The Cygwin utilities files were also used for comparison in [15, 28].

Table 3: Cygwin files from ./cygutils

Cygwin benign file	Cygwin benign file
ascii.exe	msgtool.exe
banner.exe	putclip.exe
conv.exe	readshortcut.exe
cygdrop.exe	realpath.exe
cygstart.exe	getclip.exe
dump.exe	semstat.exe
lpr.exe	semtool.exe
mkshortcut.exe	shmttool.exe

We also evaluate our method against metamorphic worms generated by MWOR [18, 19], which is a generator developed to evade statistical-based detection such as the HMM-based detector we discussed in Section 2.2.1. One of the metamorphic techniques MWOR uses is dead code insertion. The amount of dead-code added in each replication is determined by the dead-code to worm-code padding ratio. A padding ratio of 2 means that the dead-code is twice as much as the worm instructions. Additionally, the instructions used for padding are retrieved from a subset of the benign files in our test set. Insertion of dead-code allows the worm to assimilate code patterns present in benign programs. Its intent is to resemble ordinary programs

to avoid detection.

In our experiments, we use seven sets of MWOR with increasing padding ratios of 0.5, 1.0, 1.5, 2.0, 3.0, and 4.0 [24]. With higher padding ratios, the expectation is a high degree of similarity will result from worm and benign files comparison. Since the MWOR files [24] were generated on a Linux environment, for comparison, we use a set of 30 Linux system programs shown in Table 4.

Table 4: Linux system files

Linux benign file	Linux benign file
/bin/date	usr/bin/kill
/bin/dmesg	usr/bin/killall
/bin/grep	usr/bin/last
/bin/mknod	usr/bin/ld
/bin/mount	usr/bin/namei
/bin/rm	usr/bin/nm
/bin/sleep	usr/bin/nm-tool
/bin/sync	usr/bin/objdump
/bin/touch	usr/bin/oclock
/usr/bin/as	usr/bin/readelf
/usr/bin/at	usr/bin/rpl8
/usr/bin/file	usr/bin/shuf
/usr/bin/funzip	usr/bin/size
/usr/bin/dig	usr/bin/strip
/usr/bin/msgcat	usr/bin/sum

4.2 Parameters

Recall that our algorithm consists of two stages, namely, file segmentation and sequence comparison. In the file segmentation phase, we build an entropy map of a file using sliding window. We set the window size to 64 bytes for the G2 and NVGCK files, and 256 bytes for the MWOR file sets. The slide size is set to approximately

half the window size, making certain that the entropy map is of size power of 2. This size restriction is due to the segmentation algorithm, which successively splits the input data in half at each transformation scale [22]. We use lower values for G2 and NGVCK due to their small file sizes. Higher parameter values generate insufficient number of segments necessary for sequence comparison.

For computing the total penalty cost in equation (6) in the sequence comparison phase, we set the coefficients to 0.4 and 1.6 for PART_ENT and PART_SIZE, respectively. By using such values, the size difference of the compared segments is augmented. This increases the influence of the size penalty to the overall cost. The constant TAX is set to 0.3, meaning the average penalty for a pair of mismatching segments is 0.3.

4.3 Results

First, we applied our similarity measure to a family of G2 viruses and a set of Cygwin utility files. We used the process outlined at the start of this chapter. Figure 12 shows the results, where the red points correspond to the similarity percentages between virus pairs and the virus-benign pairs are denoted by the green points. You can see in this diagram that the G2 viruses are almost identical with one another. The similarity percentages are all above 95%. Since [28] found that the virus variants generated by G2 have the highest average similarity among other generators, the result here is as expected. Also, notice the three bands among the virus-benign pairs. These are formed due to the file size difference between the benign files and the viruses. The higher the size difference, the lower the similarity is between them. Evidently, our method is capable of detecting G2 viruses with false positive rate of 0%. We can easily use the lowest similarity score of a pair of viruses for setting the

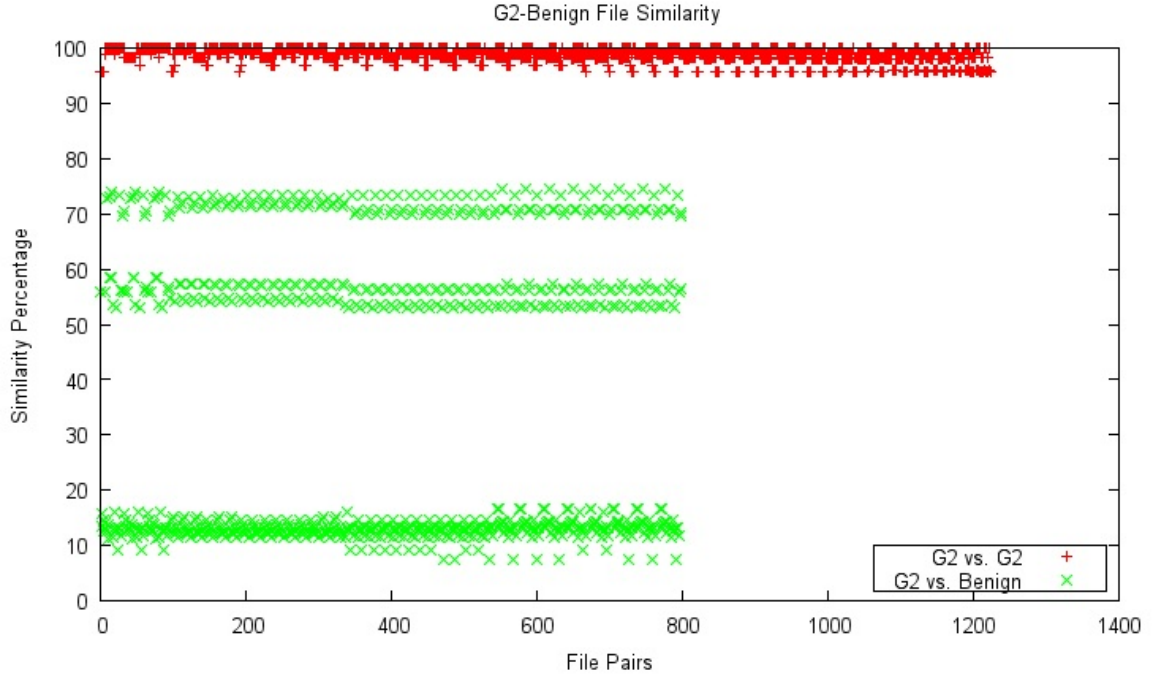


Figure 12: G2 similarity

threshold, which is 95.61%.

Next, we assessed our method against the MWOR family of metamorphic worms. We tested seven MWOR sets with differing padding ratios. Each MWOR set was compared against a set of benign programs consisting of Linux system files. Figure 13 displays the results of MWOR with 0.5 padding ratio. This ratio means that the worm samples contain half as much dead-code as the actual worm instructions. Notice the similarity results between worms and benign files, particularly the low group of points around 30% and 40%. Since different variants of the same malicious program are typically equal in size [17] and our solution penalizes on the size difference, the smallest and largest benign files scored the lowest when compared to the worm files. Also, a subset of the benign files used for padding the worm code [19] came close to the average similarity of all worm and benign files comparisons, which is around 67%.

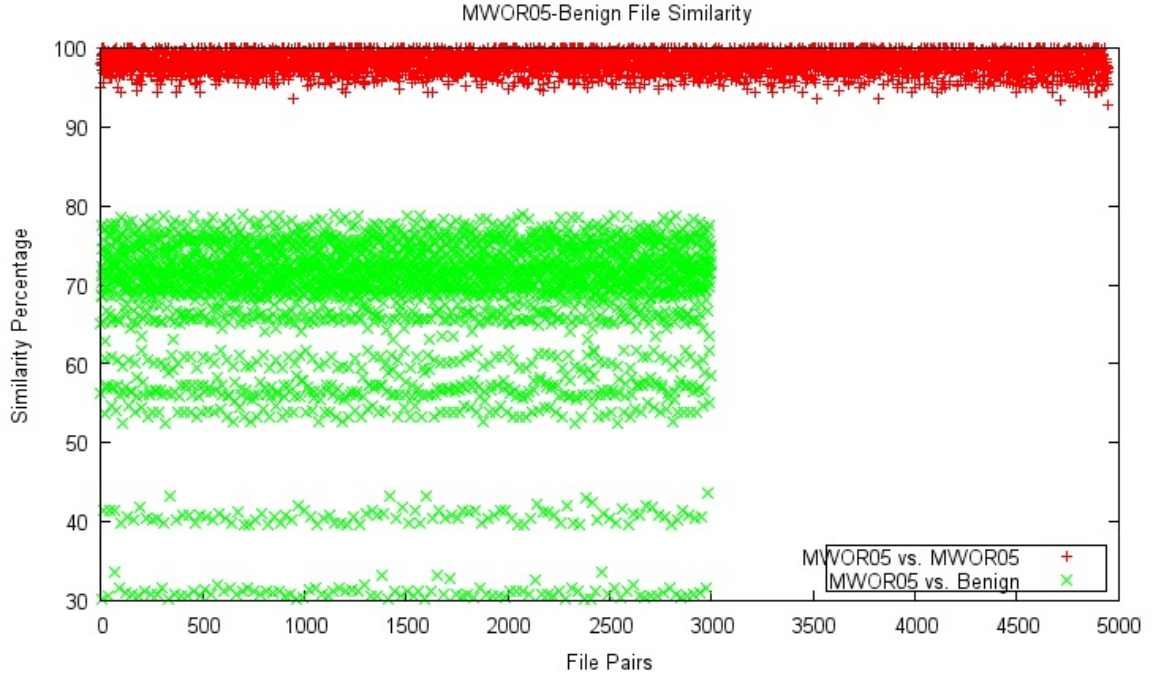


Figure 13: MWOR 0.5 similarity

The similarity percentages between the worm files are well above 90%; thus, we can set the threshold to the lowest similarity score of 92.82% without any false positive detection. The statistics of our results are summarized in Table 5.

Table 5: MWOR 0.5 similarity statistics

Comparison	Mean (%)	Minimum (%)	Maximum (%)
worm vs. worm	98.18	92.82	100
worm vs. benign	67.47	30.19	79.02

We performed the same experiments on MWOR sets with higher padding ratios and the results are consistent with the outcome from MWOR 0.5. Although the average similarity between worms decreases as the padding ratio increases, the separation between the worms and benign files is evident in every MWOR set. Therefore, our method is capable of detecting different samples of MWOR files. The similarity plots

are shown in Appendix A. Table 6 summarizes the similarity statistics of the MWOR families.

Table 6: MWOR similarity statistics

Family	Comparison	Mean (%)	Minimum (%)	Maximum (%)
MWOR 1.0	worm vs. worm	97.50	93.14	100.00
	worm vs. benign	66.63	30.50	79.61
MWOR 1.5	worm vs. worm	97.08	93.20	100.00
	worm vs. benign	68.60	24.19	78.61
MWOR 2.0	worm vs. worm	96.33	91.96	100.00
	worm vs. benign	68.72	26.73	78.49
MWOR 2.5	worm vs. worm	95.62	92.23	100.00
	worm vs. benign	68.32	24.16	77.87
MWOR 3.0	worm vs. worm	95.00	89.30	100.00
	worm vs. benign	67.68	26.06	77.87
MWOR 4.0	worm vs. worm	93.84	89.96	100.00
	worm vs. benign	65.82	27.24	78.64

Lastly, we turn to the NGVCK virus family, which [28] found to be the most highly metamorphic. Our first observation is that files in this sample differ in size. This is unlike the G2 and MWOR test data where all the files within each set have the same size. Out of the 50 NGVCK files in our test set, 34 files are 4 kilobytes in size, 13 files are 8 kilobytes, and the other three files are 16, 36, and 40 kilobytes (KB). First, we ran a similarity test between the 34 NGVCK files (4 KB) and a set of Cygwin files listed in Table 3. The plot is shown in Figure 14. While the average similarity score of the virus pairs came out high at 90.31%, there are a number of overlaps among the virus and benign file comparisons. If we take the minimum score from the virus pair comparisons and set it as the threshold, 1.5% of the virus and benign pairs score higher than the threshold.

We repeated the same test on the group of 13 NGVCK files having equal size of

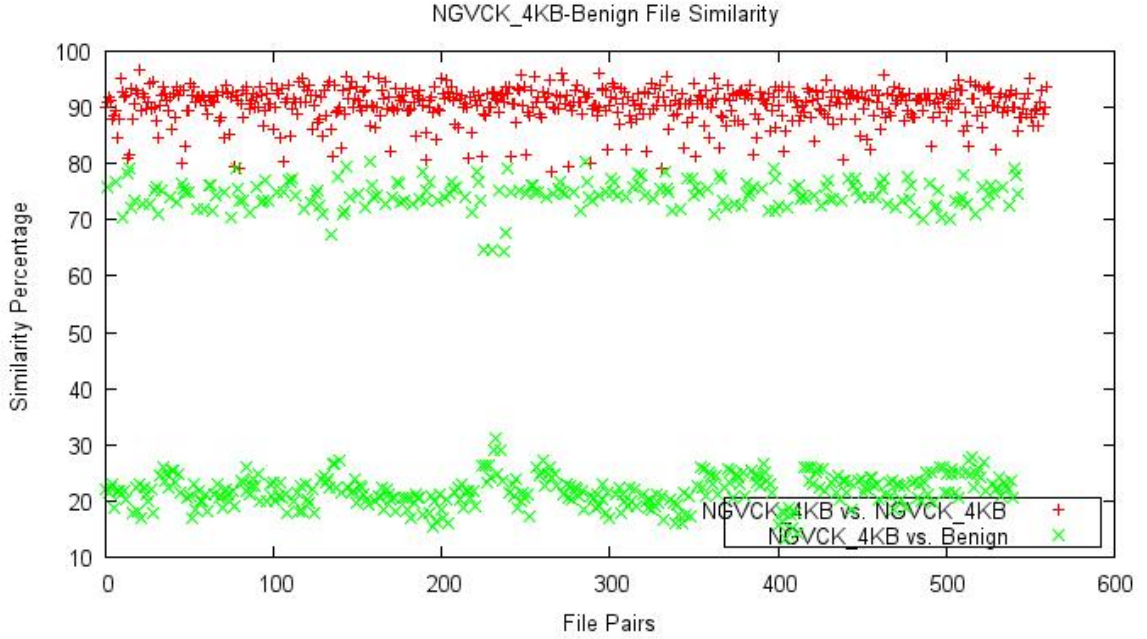


Figure 14: NGVCK (4 KB) similarity

8 KB. Figure 15 displays the similarity plot. In this case, the threshold can be set to the minimum virus pair comparison score with 0% false positive rate. However, if we combine the 4 KB and 8 KB NGVCK files, a number of virus pair comparisons result to a low degree of similarity and we are unable to set a concrete threshold. This similarity plot is shown in Figure 16. Adding the other three larger NGVCK files (16 KB, 36 KB, 40 KB) into the set produced similar result where a threshold is not tangible. The plot is included in Appendix B. Statistics of NGVCK are also presented in Appendix B.

We summarize all the results by plotting the ROC curves. An ROC (Receiver Operating Characteristics) curve is a visual aid for performance analysis of a classifier. It illustrates the trade-off between true positive rates and false positive rates for varying thresholds [6]. Figure 17 shows the ROC curves for the NGVCK results. The curves for the 4 KB and 8 KB file sets are trivial, whereas curves for the combined

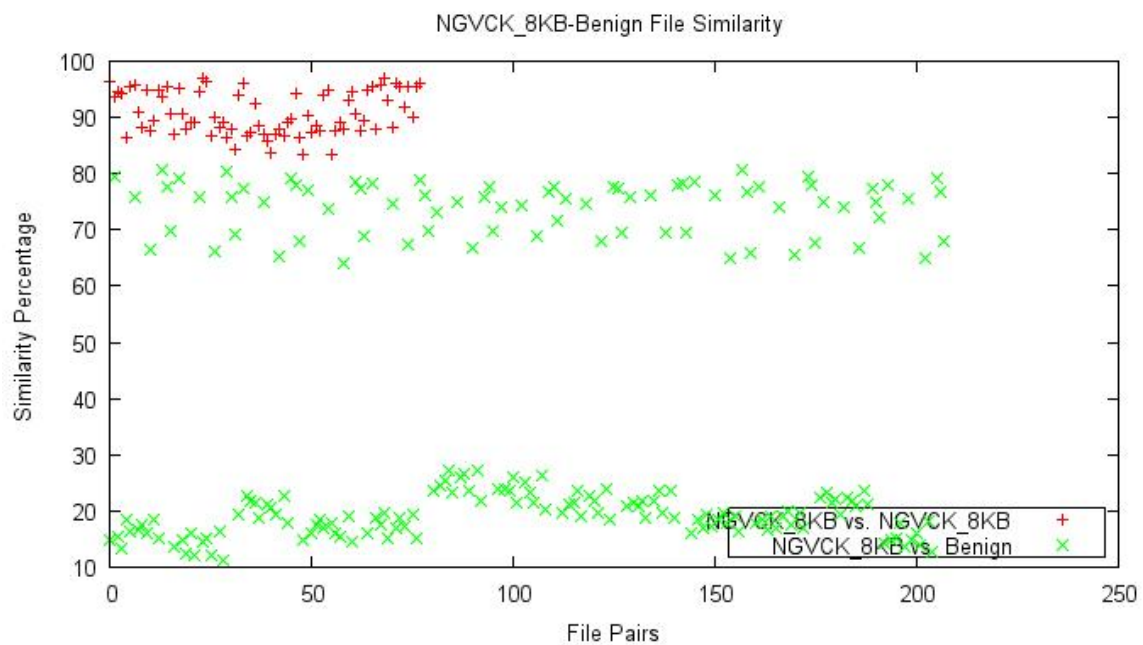


Figure 15: NGVCK (8 KB) similarity

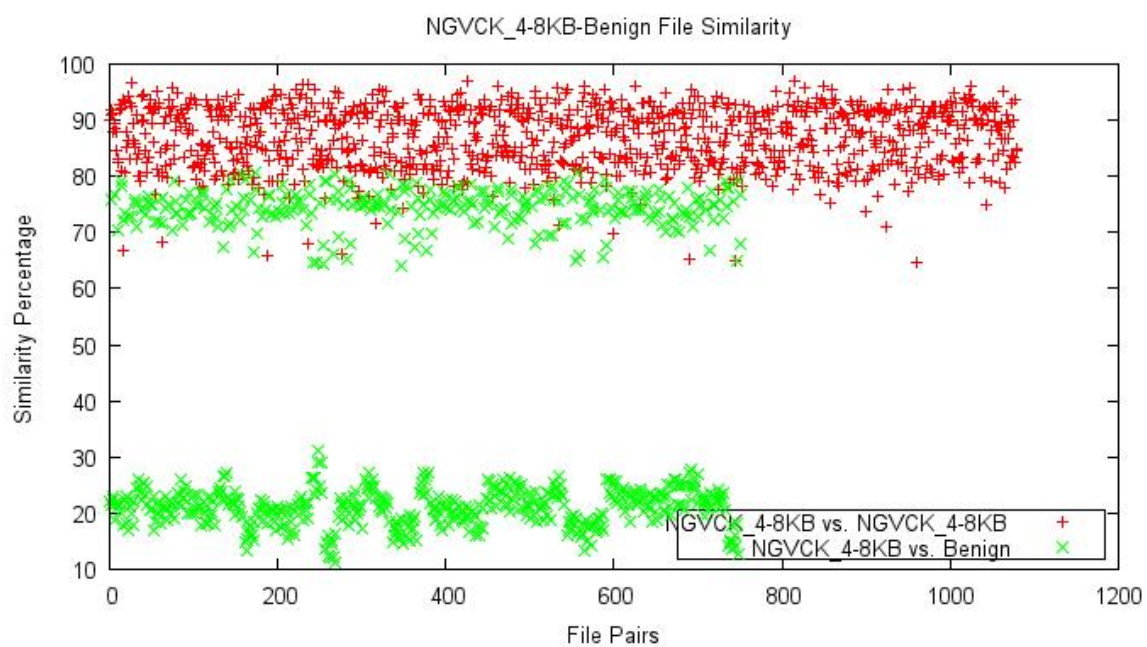


Figure 16: NGVCK (4 KB and 8 KB) similarity

sets exhibit the effect of the overlaps between viruses and benign files comparisons.

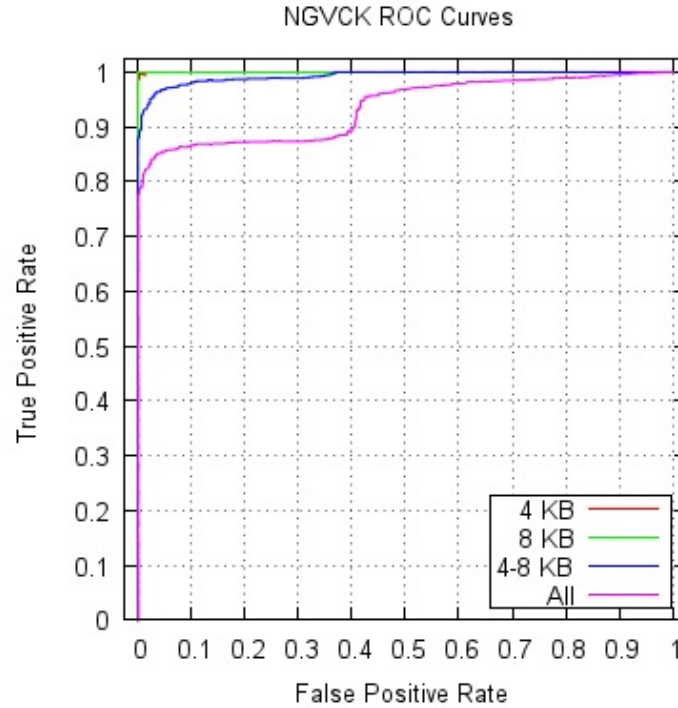


Figure 17: NGVCK ROC curves

We also calculated the area under the curve (AUC) for each of the ROC graphs. The AUC measures the accuracy of a classifier with values from 0 to 1.0, where 1.0 indicates faultless classification [6]. However, a usable classifier should have an AUC above 0.5. Otherwise, it would be no better than random guessing. Table 7 displays the AUC for sets of NGVCK files. The ROC and AUC results for G2 and MWOR

Table 7: AUC of NGVCK

NGVCK File Set	AUC
4 KB (34 files)	0.99989
8 KB (13 files)	1.00000
4-8 KB (47 files)	0.99262
All (50 files)	0.93539

are in Appedix C.

Additionally, to analyze the impact of the cost parameters, we calculated the AUC for different values of PART_ENT and PART_SIZE on the complete NGVCK file set. For the entropy parameter, we used a range of values from 0 to 1 with 0.05 increments, and values from 0 to 2 with 0.10 increments for the size parameter. Figure 18 shows the results. Notice that for any values of PART_ENT where PART_SIZE is below 0.80 and for any combination where PART_ENT is below 0.25, our method’s accuracy is 0.92 at best, which is lower than our experimental result found in Table 7 for all 50 NGVCK files. This confirms that the parameter values used in our experiments are adequate.

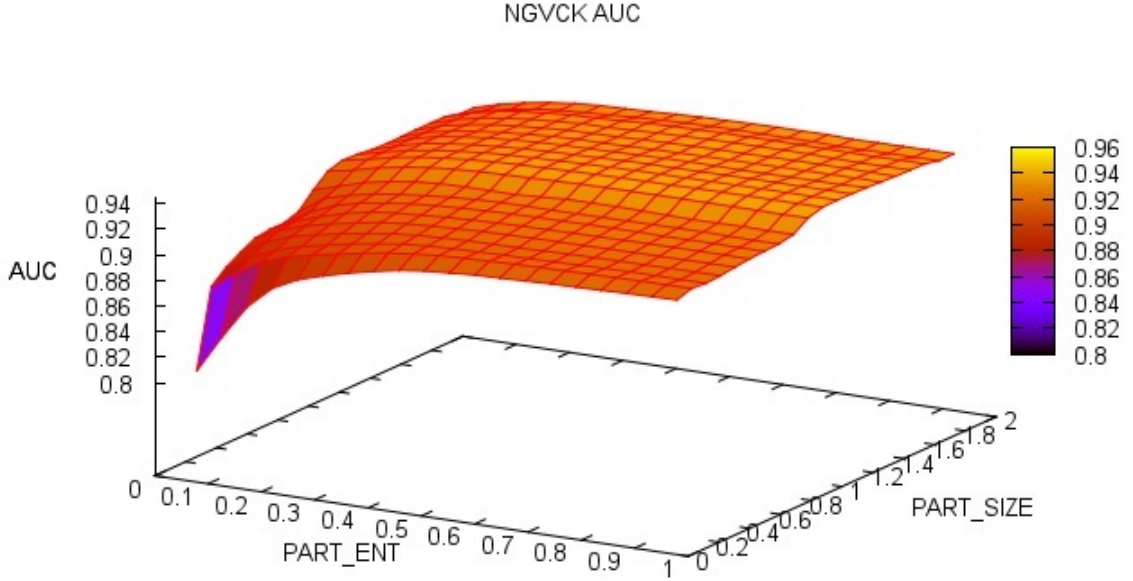


Figure 18: AUC for NGVCK with various parameter values

Finally, to determine the efficiency of our method, we processed various files with sizes ranging from 10 KB to 4 MB. For files less than 100 KB in size, the processing

time is around 0.02 seconds. A 4 MB file took less than 1 second to complete. The results are shown in Figure 19. Note that the largest malware file in our experiments is 68 KB, so each of those samples took no longer than 0.02 seconds to score. These processes times were measured on a 64-bit Windows 7 machine with Intel Core i5-2540M processor at 2.60 GHz and 8 GB of memory.

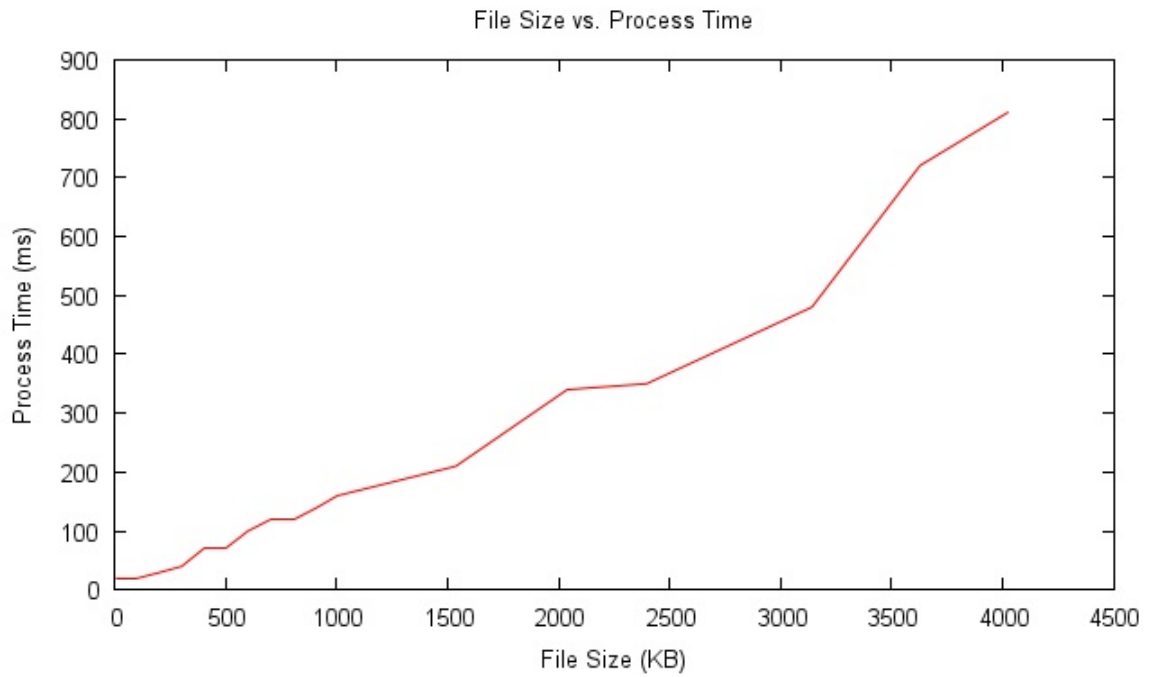


Figure 19: File processing time

CHAPTER 5

Conclusion and Future Work

The similarity method presented in this paper is based on static analysis of files. Development of such measure is vital in classification of highly metamorphic malware since it uses obfuscation techniques designed to evade signature-based detection. We reviewed other static detection schemes, which analyze opcode sequences of executable files. In contrast, our solution examines the binary files directly and evaluates the distinction of bytes within the files. Therefore, our algorithm requires no code disassembly, reducing computational overhead.

We applied our method to the metamorphic malware detection problem. The experiments show that our proposed solution is capable of identifying malware samples generated by the G2 and MWOR metamorphic generators at a 100% rate. It appears that the amount of dead-code applied by the MWOR generator in our test set did not impact the structural entropy of the worms. However, it is valuable to mention that the average similarity between MWOR files slowly decreased with increasing padding ratio. Therefore, given a sufficient amount of dead-code may strengthen its ability against static detection. Nevertheless, large blocks of instructions that never execute may appear suspicious to modern anti-virus emulators.

We repeated the same experiment against NGVCK family of viruses. Immediately, we noticed the size differences of the NGVCK files, 34 of which are 4 KB in size, 13 are 8 KB, and the other three files are 16 KB, 36 KB, and 40 KB. We grouped these files based on their sizes and ran separate tests. We also ran additional tests on combined files. Our technique was able to distinguish the viruses from the

benign programs with a tolerable 1.5% false match for the 4 KB files. The 8 KB NGVCK files resulted in 100% detection rate without false positive. In the combined test, however, a threshold was not viable. Our experiments resulted in a number of overlaps between viruses and benign files. It appears that NGVCK not only has the ability to change its structure at certain generations, it also makes some variants look more like normal programs.

Overall, our results indicate that a similarity measure based on structural entropy is potentially useful for classifying highly metamorphic malware. At the least, this creates an additional hurdle that a malware writer must clear to create metamorphic malware that is undetectable by static means.

For future work, it might be worthwhile to further study the NGVCK samples and its morphing techniques. Also, it may be worth exploring the cost function used this research. Balancing the influence of the entropy and size differences between compared elements might improve the similarity score. Furthermore, consideration of other algorithms for sequence comparison that employ local alignment may also improve the results for sequences with diverse lengths, which is the case for the NGVCK samples. Such alignment methods take into account only similar regions rather than all elements in the sequences. A well-known method based on local sequence alignment is the Smith-Waterman algorithm, which compares all possible sub-sequences and selects the optimal one [30].

LIST OF REFERENCES

- [1] P. Addison. *The Illustrated Wavelet Transform Handbook: Introductory Theory and Applications in Science, Engineering, Medicine and Finance*. Taylor and Francis Group, 2002.
- [2] A. Apostolico and Z. Galil. *Pattern Matching Algorithms*. Oxford University Press, 1997.
- [3] M. Borda. *Fundamentals in Information Theory and Coding*. Springer, 2011.
- [4] Cygwin. Cygwin utility files.
<http://www.cygwin.com/>.
- [5] Dictionary, Entropy.
<http://dictionary.reference.com/browse/entropy>.
- [6] T. Fawcett. ROC graphs: notes and practical considerations for researchers. Bioinformatics and Computational Biology, George Mason University, 2004.
<http://binf.gmu.edu/mmasso/ROC101.pdf>.
- [7] R. Islam, A. W. Naji, A. A. Zaidan, and B. B. Zaidan. New system for secure cover file of hidden data in the image page within executable file using statistical steganography techniques. *International Journal of Computer Science and Information Security (IJCSIS)*, Vol. 7, No. 1, pp. 273-279, January 2010.
- [8] Karmeshu. *Entropy Measures, Maximum Entropy Principle and Emerging Applications*. Springer, 2003.
- [9] S. Kazi, Hidden markov models for software piracy detection, Master's report, Department of Computer Science, San Jose State University, 2012.
http://scholarworks.sjsu.edu/etd_projects/236/.
- [10] Wikipedia. Levenshtein distance, 2012.
http://en.wikipedia.org/wiki/Levenshtein_distance.
- [11] SearchSecurity. Metamorphic and polymorphic malware, 2010.
<http://searchsecurity.techtarget.com/definition/metamorphic-and-polymorphic-malware>.
- [12] M. Patel, Similarity tests for metamorphic virus detection, Master's report, Department of Computer Science, San Jose State University, 2011.
http://scholarworks.sjsu.edu/etd_projects/175/.

- [13] M. Pietrek. Peering inside the PE: a tour of the Win32 portable executable file format. *MSDN Magazine*
<http://msdn.microsoft.com/en-us/magazine/ms809762.aspx>.
- [14] S. Robinson. *Expert .NET 1.1 Programming*. Apress, 2004.
- [15] N. Runwal, R. Low, and M. Stamp, Opcode graph similarity and metamorphic detection. *Journal in Computer Virology*, Vol. 8, No. 1-2, pp. 37-52, May 2012.
- [16] A. Singh. *Identifying Malicious Code Through Reverse Engineering*. Springer, 2009.
- [17] I. Sorokin. Comparing files using structural entropy. *Journal in Computer Virology*, Vol. 7, No. 4, pp. 259-265, November 2011.
- [18] S. M. Sridhara. Metamorphic worm that carries its own morphing engine. Master's report, Department of Computer Science, San Jose State University, 2012.
http://scholarworks.sjsu.edu/etd_projects/240/.
- [19] S. M. Sridhara and M. Stamp. Metamorphic worm that carries its own morphing engine. *Journal in Computer Virology*, October 2012.
- [20] M. Stamp, A revealing introduction to hidden Markov models, 2012,
<http://cs.sjsu.edu/~stamp/RUA/HMM.pdf>.
- [21] Z. Struzik and A. Siebes. The haar wavelet transform in the time series similarity paradigm. In *Proceedings of the Third European Conference on Principles of Data Mining and Knowledge Discovery* (PKDD '99). Springer-Verlag, London, UK, 12-22.
<http://dl.acm.org/citation.cfm?id=669368>.
- [22] P. Van Fleet, The discrete haar wavelet transformation, Joint Mathematical Meetings, Center for Applied Mathematics, University of St. Thomas, 2007,
[http://cam.mathlab.stthomas.edu/wavelets/pdf/files/
NewOrleans07/HaarTransform.pdf](http://cam.mathlab.stthomas.edu/wavelets/pdf/files/NewOrleans07/HaarTransform.pdf).
- [23] G. Verschuuren. *Excel 2007 for Scientists and Engineers*. Holy Macro! Books, 2008.
- [24] Department of Computer Science, San Jose State University. Virus files, 2012.
<http://cs.sjsu.edu/~stamp/viruses/>.
- [25] Symantec. Viruses, worms, and trojans, 2011.
<http://service1.symantec.com/support/nav.nsf/docid/1999041209131106>.

- [26] T. Vuorenmaa, The discrete wavelet transform with financial time series applications, Seminar on Learning Systems, University of Helsinki, 2003. http://www.rni.helsinki.fi/teaching/sols/TV_RNI.pdf.
- [27] R. A. Wagner and M. J. Fischer. The string-to-string correction problem. *Journal of the ACM (JACM)*, Vol. 21, No. 1, pp. 168-173, January 1974.
- [28] W. Wong and M. Stamp, Hunting for metamorphic engines. *Journal in Computer Virology*, Vol. 2, No. 3, pp. 211-229, December 2006.
- [29] I. You and K. Yim, Malware obfuscation techniques: a brief survey. *Broadband, Wireless Computing, Communication and Applications (BWCCA), 2010 International Conference on*, pp. 297-300, November 2010.
- [30] M. Zvelebil and J. O. Baum. *Understanding Bioinformatics*. Garland Science, Taylor & Francis Group, 2008.

APPENDIX A

MWOR Results

Figures A.20, A.21, A.22, A.23, A.24 and A.25 show the similarity plots of MWOR family of worms with padding ratios 1.0, 1.5, 2.0, 2.5, 3.0, and 4.0, respectively. Each MWOR set was compared with a set of benign files listed in Table 4 of Section 4.1.

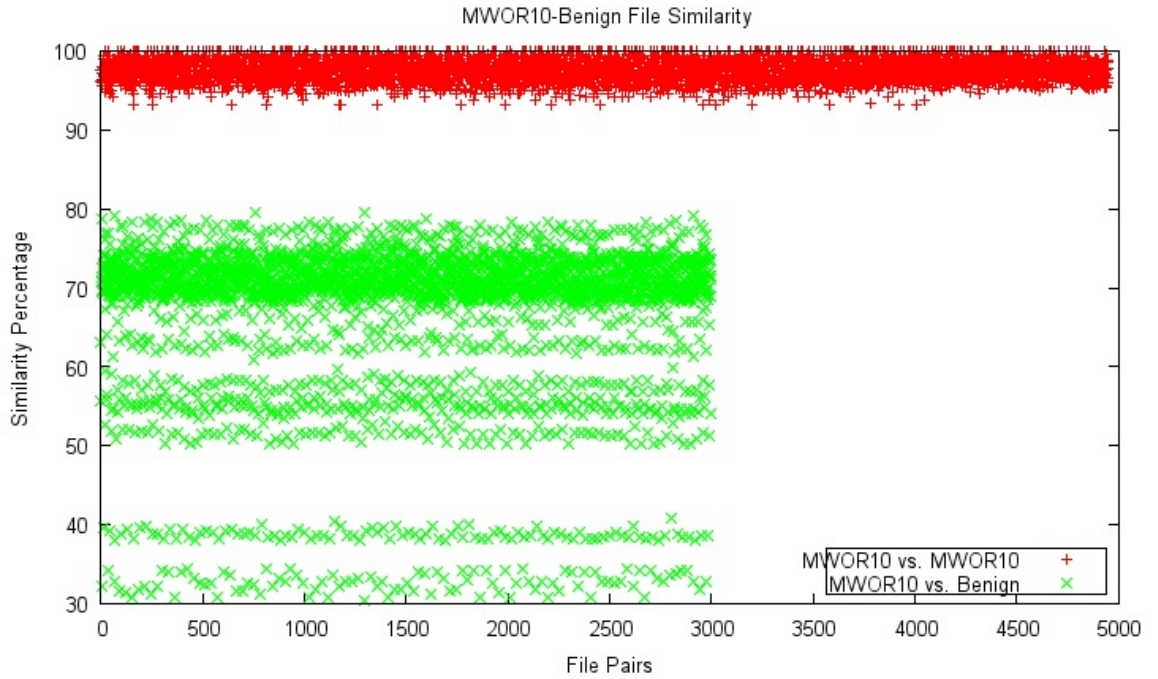


Figure A.20: MWOR 1.0 similarity

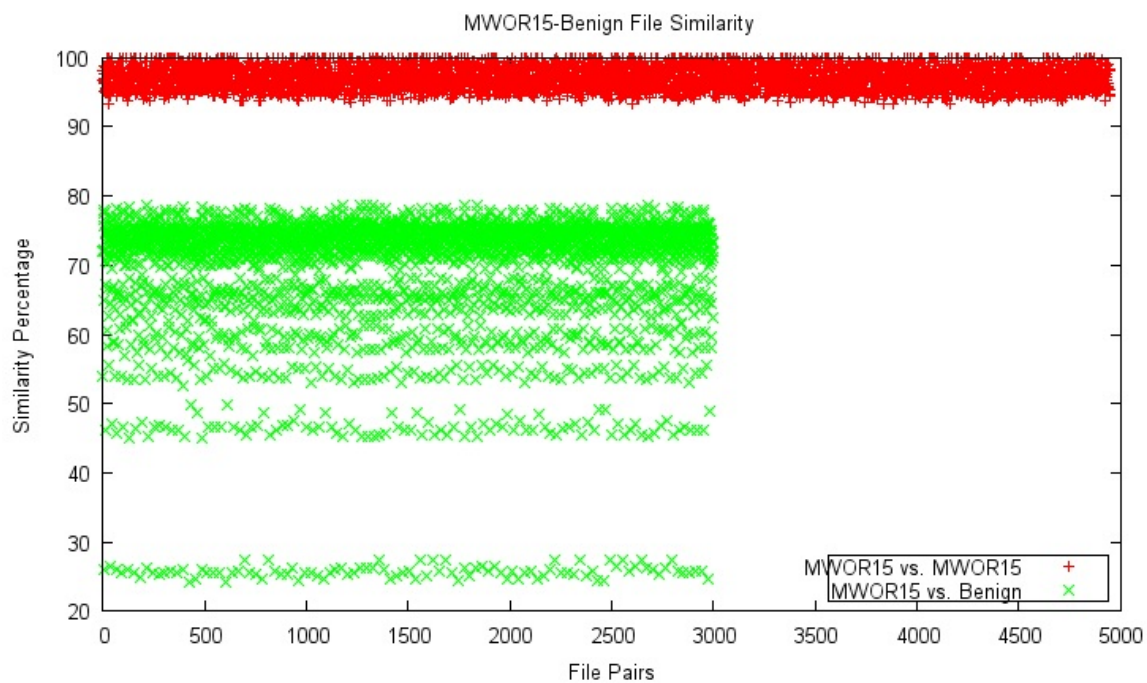


Figure A.21: MWOR 1.5 similarity

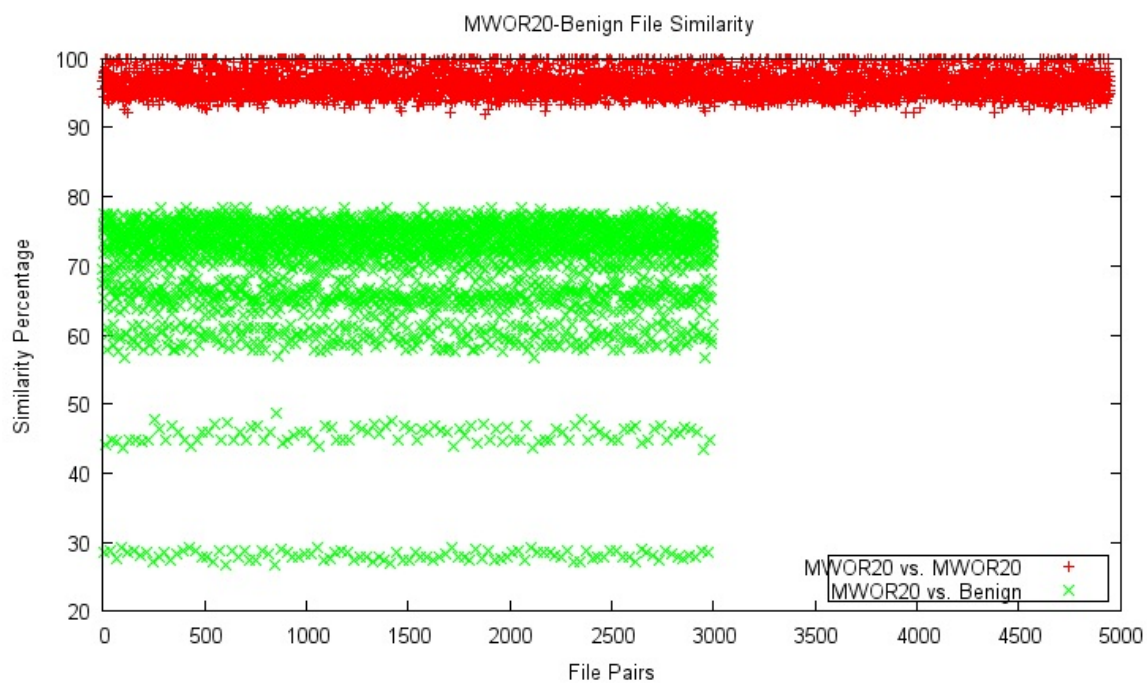


Figure A.22: MWOR 2.0 similarity

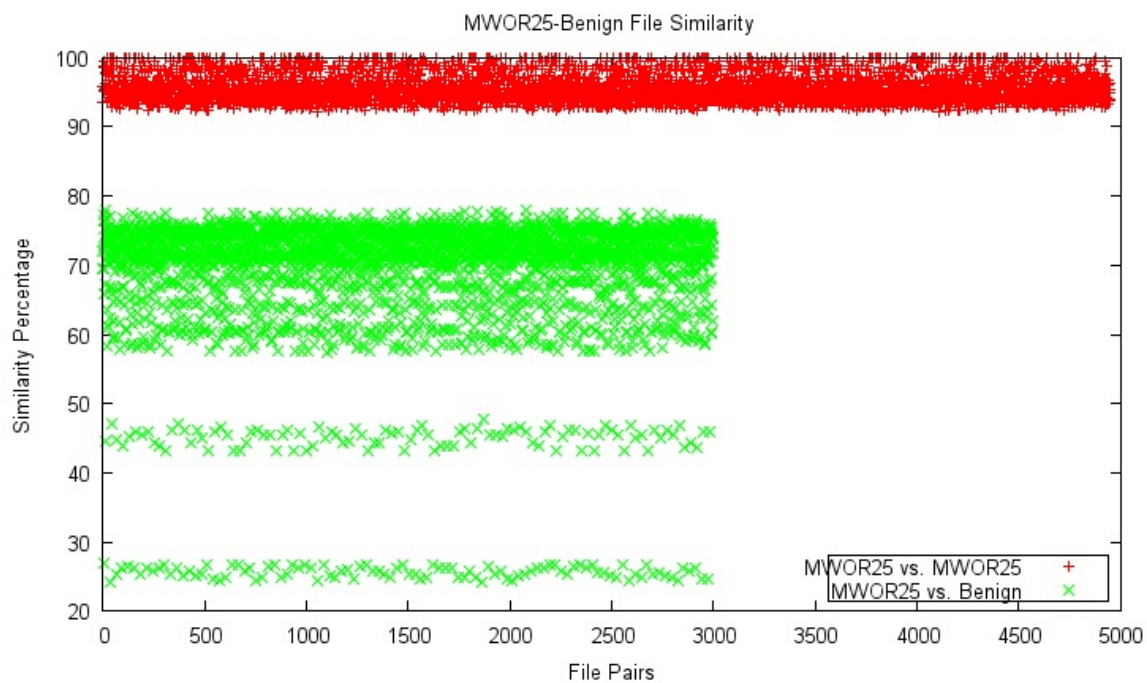


Figure A.23: MWOR 2.5 similarity

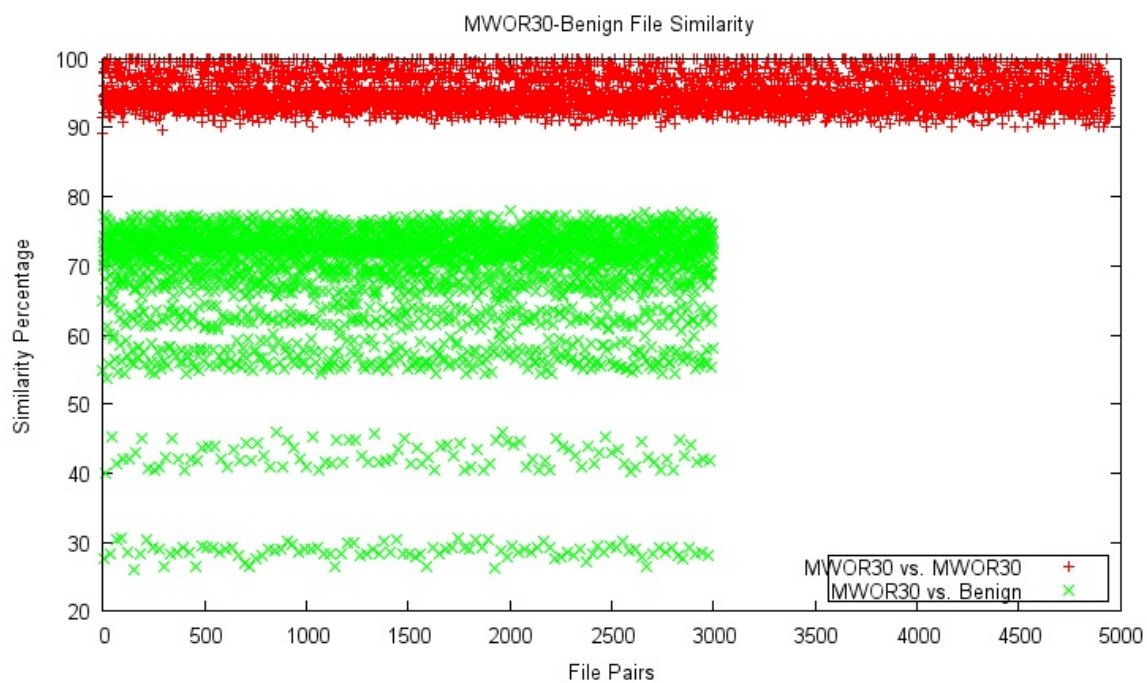


Figure A.24: MWOR 3.0 similarity

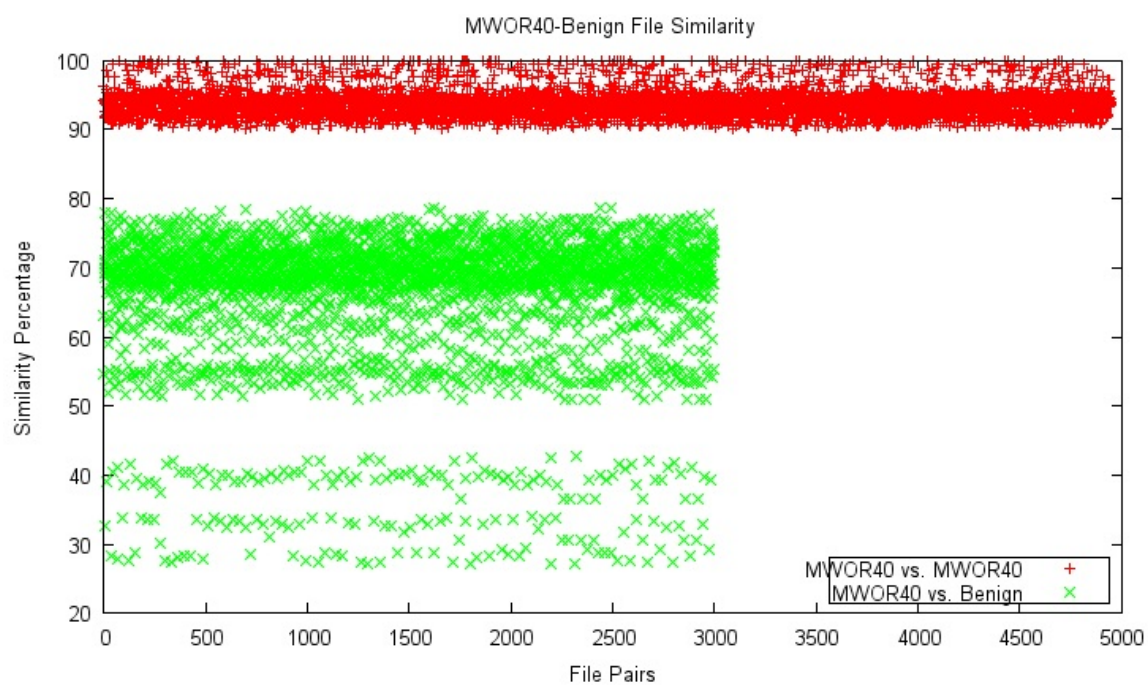


Figure A.25: MWOR 4.0 similarity

APPENDIX B

NGVCK Results

Figure B.26 shows the similarity plot for all 50 NGVCK files. The statistics for the NGVCK sets are in Table B.8.

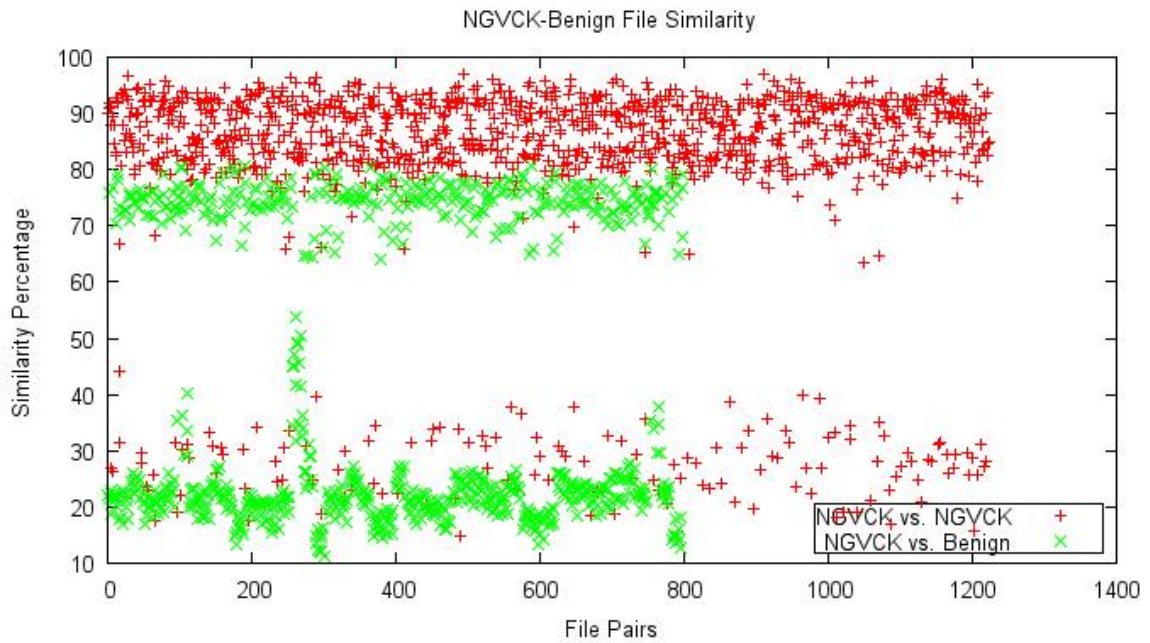


Figure B.26: NGVCK similarity

Table B.8: NGVCK similarity statistics

Family	Comparison	Mean (%)	Minimum (%)	Maximum (%)
NGVCK (34 4KB files)	worm vs. worm	90.31	78.63	96.58
	worm vs. benign	41.61	13.47	80.26
NGVCK (13 8KB files)	worm vs. worm	90.79	83.36	96.88
	worm vs. benign	39.71	11.40	80.61
NGVCK (4KB + 8KB files)	worm vs. worm	86.91	64.72	96.88
	worm vs. benign	41.09	11.40	80.61
NGVCK (all 50 files)	worm vs. worm	80.08	15.00	96.88
	worm vs. benign	41.84	11.40	80.61

APPENDIX C

ROC Curves

Figure C.27 shows the ROC curve for G2 with AUC of 1.0. The results from the MWOR experiments all produced the same ROC curve, which is shown in Figure C.28 with AUC of 1.0.

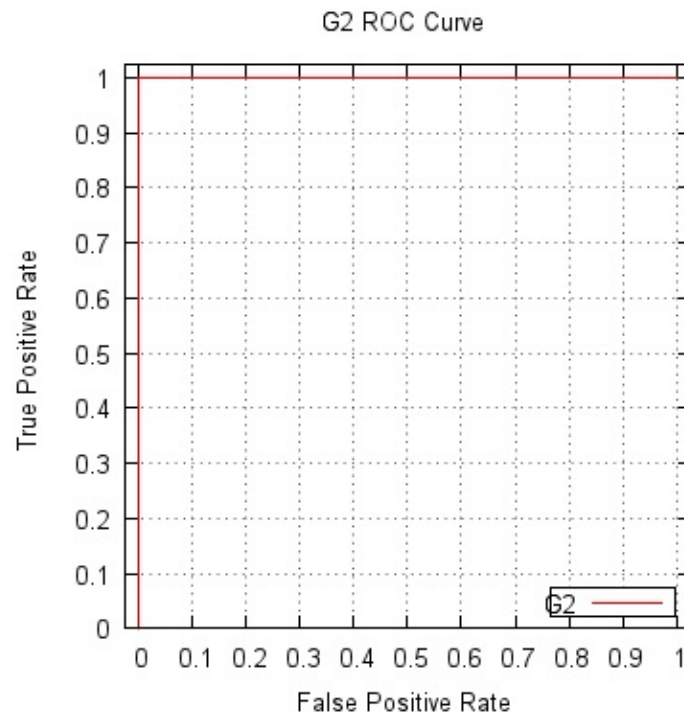


Figure C.27: G2 ROC curve

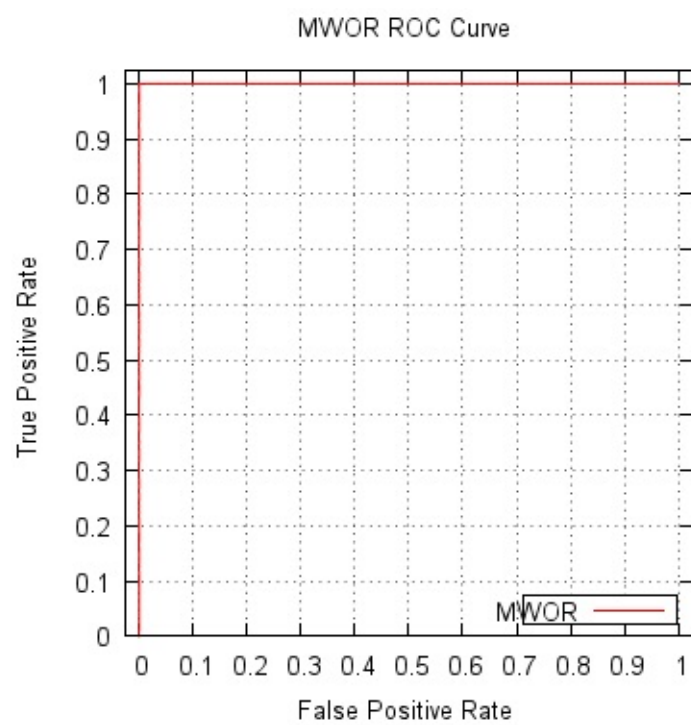


Figure C.28: MWOR ROC curve (for all padding ratios)